Article

WIND ENGINEERING

Wind Engineering
1–23

DOI: 10.1177/0309524X18814966
journals.sagepub.com/home/wie
SAGE

Wind capacity growth in the Northwest United States: Cooptimized versus sequential generation and transmission planning

Patrick Maloney[1], Ping Liu[1], Qingyu Xu[2], James D McCalley[1], Benjamin F Hobbs[2], Sara Daubenberger[3], Anders Johnson[3] and Stan Williams[3]

Abstract
This article demonstrates the benefits of simultaneous cooptimization on a 312-bus network representation of the Western Interconnection power grid with emphasis on The Bonneville Power Administration's operational area in the Pacific Northwest. While generation and transmission expansion planning has traditionally been solved sequentially, simultaneous cooptimization of both guarantees plans at least as cost effective as sequential approaches and better integrates high-quality remote resources like wind into power grids. For three scenarios with varied carbon and transmission costs, results indicate that (1) simultaneous cooptimization provides up to 6 billion dollars in net present value benefits over sequential optimization during the 50-year planning horizon, (2) cooptimization is more adept at tapping into superior remote resources like wind that the sequential approach has trouble identifying for low iterations, and (3) 10 iterations of sequential cooptimization only capture 75%–96% of the transmission benefits of simultaneous cooptimization.

Keywords
Generation expansion planning, transmission expansion planning, cooptimization, long-term planning, wind power

Introduction

Cooptimization of generation and transmission investment represents a new long-term planning paradigm for effective planning of the bulk electric power grid. Traditionally, planning new generation and transmission resources has occurred in sequence with the more expensive generation planning occurring first. However, planning in sequence may not detect solutions consisting of certain combinations of transmission and generation. Generation and transmission cooptimization overcomes the shortcoming of sequential planning by considering all possible combinations of generation and transmission resources simultaneously in the same optimization formulation. As a result, the cooptimization planning approach will always develop a model at least as cost effective as the sequential approach because it considers excellent remote resources that may outperform local resources despite expensive transmission upgrades.

The purpose of this work is to quantify the value of cooptimization as well as its importance to the magnitude of remote wind investment and transmission investments within a 19-year generation and transmission cooptimization capacity expansion planning problem. Historically, generation and transmission planning has been done in sequence for a variety of reasons. Institutional reasons for why the planning processes are done separately include the following:

1. Generation per MW is much more expensive than transmission so it is often planned first, and appropriate transmission decisions follow;

[1]Iowa State University, Ames, IA, USA
[2]Johns Hopkins University, Baltimore, Maryland, USA
[3]The Bonneville Power Administration, Portland, OR, USA

Corresponding author:
James D McCalley, Iowa State University, Ames, IA 50011, USA.
Email: jdm@iastate.edu

2. Different utilities often own the generation and transmission assets in the electric power sector which makes coordinated planning efforts more difficult.

In addition, generation and transmission are often planned for separately as modeling both in the same mathematical formulation is generally much more computationally intensive.

However, generation and transmission planning is, to some extent, substitutable. By building generation, new resources are connected to the grid that can service loads using the existing network. Additional transmission also achieves this by increasing the capacity of branches within the network and allowing underutilized or even cheaper resources to service loads from a distance. A primary benefit to planning for both generation and transmission resources simultaneously is that it can reduce infrastructure investment and operational costs resulting in lower energy costs.

In the Northwest United States, wind resource quality tends to improve with distance from the load centers on the coast, with the highest capacity factor resources available to the Northwest being located in Montana and Wyoming. In order to determine the benefits of cooptimization for the Northwest region, this work compares the effect of simultaneously cooptimizing generation and transmission as opposed to using the traditional sequential optimization of generation followed by transmission.

The remainder of this article is organized as follows. The literature review includes a discussion of literature building up to the most recent uses of cooptimization benefit quantification is provided. Next, the model formulation and simulation methods are described. Results, discussion of results, and study conclusions, follow.

Literature review

Initial efforts at using mathematical programming techniques have focused on solving the generation and transmission expansion problems separately. According to Adams et al. (1972), an early effort at using mathematical optimization for capacity expansion planning is found in Masse and Gibrat (1957). This work minimizes the total cost of a generation expansion plan (GEP) subject to a constraint on investment costs. The plan evaluates several types of hydro-, tidal, and steam power plants and determines that for different allotted investment cost budgets different combinations of candidate plants represent the most economic plans. Extensions to linear programming as a planning tool using load duration curves are discussed in Adams et al. (1972) and Berrie and Anderson (1972) which are summarized by Sasson and Merrill (1974). While both Adams et al. (1972) and Berrie and Anderson (1972) discuss linear programming techniques for GEP, Adams et al. (1972) go one step further by introducing the concept of transmission expansion planning (TEP) using a transportation model. In Garver (1970), an application of the TEP is solved using linear programming techniques on a six-bus system "to meet a specific load" (Sasson and Merrill, 1974) meaning that no load duration curve is used.

Later approaches such as Gu et al. (2012) have attempted to coordinate the GEP and TEP within an iterative procedure rather than within the same optimization formulation. This may improve solution time by decomposing and solving the GEP and TEP problems separately. However, as shown in Liu et al. (2013) (as cited in Spyrou et al. (2017)), iterative approaches may not guarantee the same optimal value that cooptimization within a single optimization problem does.

While the previously discussed studies have all been deterministic, a variety of works implement cooptimization with stochastic models. In Munoz et al. (2014), the authors focus on a detailed scenario analysis, quantify the cost of ignoring uncertainty, and emphasize the importance of rigorous stochastic planning techniques over heuristics. In Liu et al. (2017), multistage stochastic programming is implemented using a decomposition algorithm for improved computational performance. In Maloney et al. (2016), a variation on traditional stochastic programming is compared to traditional approaches, and in Maloney and McCalley (2017) the effects of wind uncertainties on the stochastic program are investigated in the context of cooptimization.

As discussed in Spyrou et al. (2017), there appears to be a lack of literature quantifitying the benefits of techniques like cooptimization over traditional approaches. She indicates that cooptimization literature tends to focus on modeling techniques within the cooptimization framework rather than on quantifying the effect of cooptimization itself. Only two works specifically focus on quantifying the benefits of cooptimization on generation and transmission expansion planning. As indicated in Spyrou et al. (2017), the paper by Liu et al. (2013) investigates cooptimization on a 13-bus representation of the US power grid, of which only three nodes are used to represent the Western Interconnection (WI). In Spyrou et al. (2017), the benefits of cooptimization are quantified for the Eastern Interconnection on a 24-bus system.

The contributions of this article are as follows: (1) this work attempts to quantify the benefit of cooptimization on a much larger and more granular network representation than has previously been attempted in Liu et al. (2013) or Spyrou et al. (2017). This work utilizes a 312-bus network representation of the WI, of which 96 buses represent the Bonneville Power Administration (BPA) area; (2) because the network is much larger and granular, it attempts to analyze investments

Table 1. Classification of generator types as dispatchable, curtailable, candidate, and existing.

Technology	G^{disp}	G^{curt}	G^{cand}	G^{exist}
Coal	×			×
Gas CCGT	×			×
Gas CT	×			×
Geothermal	×			×
Hydro		×		×
Motor load (ml)				×
Nuclear	×			×
Petroleum	×			×
PS-Hydro (ps)				×
Utility PV (fixed tilt)		×		×
Utility PV (tracking)		×		×
Solar thermal		×		×
Steam turbine	×			×
Wind onshore		×		×
Biomass	×		×	
Gas CCGT′	×		×	
Gas CT′	×		×	
Geothermal′	×		×	
Utility PV′ (fixed tilt)		×	×	
Wind onshore′		×	×	

CCGT: combined cycle gas turbine; CT: combustion turbine; PV: photovoltaic; PS: pumped storage.

and costs between the cooptimized and iterative approaches on three different levels—the WI system, the BPA operational area, and by state/region; and finally (3) while Liu et al. (2013) model Kirchhoff's Voltage Law (KVL) via a direct current (DC) power flow intra-regionally, Spyrou et al. (2017) do not consider KVL. However, Spyrou et al. (2017) observe the effect of sensitivities on the cooptimization/iterative approach methods, while Liu et al. (2013) do not. This work uses KVL for existing lines and explores the sensitivity of cooptimization and iterative approaches to both carbon and transmission costs.

Model formulation

This section defines the model elements, objective function, and constraints used to design the long-term plans illustrated in section "Results." The model borrows elements from the publicly available JHSMINE formulation (Xu and Hobbs, 2017) and was developed collaboratively with Johns Hopkins University. Table 1 defines different model technologies as dispatchable, curtailable, candidate, and existing. These definitions are used in the model to identify the manner in which the technology will be treated.

Indices

b, b' : bus

y, y' : year $y \in \{2014, 2020, 2026, 2032\}$

p : operational block

$g_{gn,b,gt}$: generator with name gn at bus b with technology gt

g : shorthand for $g_{gn,b,gt}$.
Used when generator attributes not important

gt : generation technology

$l_{b,b'}$: line from b to b'

l : shorthand for $l_{b,b'}$. Used when b,b′ order is not important

q : paths

f : fuels

n : lines bundle number $n \in \{1,2,3,4\}$
with 2^{n-1} identical lines

Sets

L_l : set of all lines l

$L_l^E \subset L_l$: existing lines

$L_{l'}^{Eq} \subset L_l^E$: network reduction equivalenced segment

$L_l^{Ep} \subset L_l^E$: network reduction preserved segment adhereing to KVL

$L_{l'}^{Ep} \subset L_l^E$: network reduction preserved segment not adhereing to KVL

$L_l^C \subset L_l$: non-KVL adhereing candidate lines

L_D^{Path} : path direction

G : set of all generators in g

$\mathrm{G}^{exist} \subset \mathrm{G}$: set of existing generators

$\mathrm{G}^{cand} \subset \mathrm{G}$: set of candidate generators

$\mathrm{G}^{disp} \subset \mathrm{G}$: set of dispatchable generators

$\mathrm{G}^{curt} \subset \mathrm{G}$: set of curtailable generators

$\mathrm{G}_{curt}^{exist} \subset \mathrm{G}^{exist}$: set of existing curtailable generators

$\mathrm{G}_{disp}^{exist} \subset \mathrm{G}^{exist}$: set of existing dispatchable generators

$\mathrm{G}_{curt}^{cand} \subset \mathrm{G}^{cand}$: set of candidate curtailable generators

$\mathrm{G}_{disp}^{cand} \subset \mathrm{G}^{cand}$: set of candidate dispatchable generators

Y : set of all years

N : set of all bundle numbers n

B : set of all buses

$B' \subset B$: set of all buses in BPA

$B'' \subset B$: set of all buses not in BPA

Parameters

P_D : value of lost load penalty

P_R : reserve shortage penalty

P_C : generation curtailment penalty

$hr_{y,p}$: number of hours in operational block

$Pd_{b,y,p}$: demand at bus b in year y, period p

$HR_{g,b,gt}$: heat rate

$CF_{b,gt,y,p}$: existing curtailable generation characteristic output

$CF'_{b,gt,y,p}$: candidate curtailable generation characteristic output

$CF''_{b,gt,y,p}$: motorload and pumped storage characteristic output

X_l : existing line l reactance

$C^{FOM}_{g,b,gt}$: fixed O&M costs

$C^{VOM}_{g,b,gt}$: variable O&M costs

$C^{Fuel}_{gt,f,y,p,b}$: fuel price

C^{Carb}_{y} : national carbon tax in year y

C^{Emis}_{gt} : emission weight per unit energy for technology gt

$D^{Peak}_{b,y}$: peak demand in year y at bus b

$G^{param}_{g,b,gt,y}$: parameterized existing generation capacity

ξ_y : discount factor without end-horizon effects

ξ'_y : discount factor with end-horizon effects

C_l : cost of full transmission line

$C_{g,b,gt,y}$: generator capital cost

CC_{gt} : capacity credit of technology gt

R_m : reserve margin (0.15)

1_x : logical operator equal to1 if x is true; 0 if false

$G^{max}_{g,b,gt,y}$: generation resource capacity limit operation

d : delay between capacity build decision and operation

r : real discount rate (0.05)

$f^{Max}_{l_{b,b'}}$: maximum line flow from b to b' on l

$f^{Min}_{l_{b,b'}}$: minimum line flow from b to b' on l

$f_q^{path,max}$: maximum path flow

$f_q^{path,min}$: minimum path flow

$f_{l_{b,b'},q}^{dir}$: direction of path $\in \{1,-1\}$

Positive continuous decision variables

C_D^{Shed} : total cost of load shedding

C_{RS}^{Shed} : total cost of reserve shortage

C_D^{Curt} : total cost of curtailment

$C_{\Delta L}$: non-KVL adhering line expansion cost

$C_{\Delta L'}$: KVL adhereing line expansion cost

$C_{\Delta G}$: total generation expansion cost

C_{FOM} : total FOM cost

C_{VOM} : total VOM cost

C^{Fuel} : total fuel cost

C_{Carb} : total carbon cost

$D_{b,y,p}^{Shed}$: load shedding

$D_{y,g,b,gt}^{Curt}$: curtailable generation curtailment

$\Delta G_{g,b,gt,y}$: new generator invested capacity

$\Delta L_{l,y,n}$: non-KVL adhereing line investment

$\Phi_{g,b,gt,y,p}$: curtailed generation

η_y : reserve shortage

Free continuous decision variables

C_{Tot} : total cost of plan

$G_{g,b,gt,y}$: cumulative generation capacity

$Pg_{g,b,gt,y,p}$: generator power output

$f_{l_{b',b},y,p}$: existing transmission line flows

$f'_{l_{b',b},y,p,n}$: candidate transmission line flows

$\theta_{b,y,p}$: phase angle

$f_{q,y,p}^{path}$: path flow

Objective

Equations (1) and (2) define the cost minimization over the objective function's nine terms. The first three terms of equation (2) are described by equations (3) to (5) and represent penalties for shedding load, missing capacity reserve requirements, and curtailing variable generation. The next two terms of equation (2) are described by equations (6) and (7) and represent the cost of building new transmission lines and generators, respectively. The last four terms of equation (2) defined in equations (8) to (11), respectively, represent the costs associated with operating the system

Objective minimization

$$\min C_{Tot} \tag{1}$$

Objective function

$$\begin{aligned} C_{Tot} &= C_D^{Shed} + C_{RS}^{Shed} + C_D^{Curt} + C_{\Delta L} \\ &\quad + C_{\Delta G} + C_{FOM} + C_{VOM} + C_{Fuel} + C_{Carb} \end{aligned} \tag{2}$$

Load shedding

$$C_D^{Shed} = \sum_{b,y,p} \xi_y \xi'_y P_D D_{b,y,p}^{Shed} hr_{y,p} \tag{3}$$

Reserve shortage

$$C_{RS}^{Shed} = \sum_{y} \xi_{\mathbf{y}} \xi'_{\mathbf{y}} \mathbf{P_R} \eta_{\mathbf{y}} \tag{4}$$

Curtailment

$$C_D^{Curt} = \sum_{y,g,b,gt} \xi_y \xi'_y P_C D_{y,g,b,gt}^{Curt} hr_{y,p} \tag{5}$$

Non-KVL adhereing line investment costs

$$C_{\Delta L} = \sum_{l \in L^C, y, n} \xi_y C_l 2^{n-1} \Delta L_{l,y,n} \tag{6}$$

Generation build costs

$$C_{\Delta G} = \sum_{g,b,gt,y} \xi_y C_{g,b,gt,y} \Delta G_{g,b,gt,y} \tag{7}$$

Fixed O&M costs

$$C_{FOM} = \sum_{g,b,gt,y} \xi_y \xi'_y C_{g,b,gt}^{FOM} G_{g,b,gt,y} \tag{8}$$

VO&M costs

$$C_{VOM} = \sum_{g,b,gt,y,p} \xi_y \xi'_y C_{g,b,gt}^{VOM} hr_{y,p} Pg_{g,b,gt,y,p} \tag{9}$$

Fuel costs

$$C_{Fuel} = \sum_{g,b,gt,y,p,f} \xi_y \xi'_y C_{gt,f,y,p,b}^{Fuel} HR_{g,b,gt} hr_{y,p} Pg_{g,b,gt,y,p} \tag{10}$$

Carbon costs

$$C_{Carb} = \sum_{g,b,gt,y,p,f} \xi_y \xi'_y C_y^{Carb} C_{gt}^{Emis} HR_{g,b,gt} hr_{y,p} Pg_{g,b,gt,y,p} \tag{11}$$

Constraints

Generation capacity. Generation modeling begins in equations (12) to (15) which track capacity and limit investments. With the exception of motor load, generation technology capacities are positive. Motor load capacity is defined as a negative capacity so that when multiplied by its characteristic output in equation (18) it is negative, indicating power consumption. Equation (15) sets a limit on the amount of investment that can be made in a candidate generator through the planning horizon at a particular bus

$$G_{g,b,gt,y'} = G_{g,b,gt,y'}^{param} + \sum_{y<y'} (\Delta G_{g,b,gt,y-d}) \quad \forall g, b, gt, y' \tag{12}$$

$$G_{g,b,gt,y} \geq 0 \text{ for } gt \neq ml \tag{13}$$

$$\Delta G_{g,b,gt,y} = 0 \text{ if } y = max(y) \quad \forall g, b, gt \tag{14}$$

$$\sum_y \Delta G_{g,b,gt,y} \leq G_{g,b,gt,y}^{max} \quad \forall g, b, gt \tag{15}$$

Generation output constraints. Operations equations (16) to (18) determine power output for curtailable generation, motor load, and pumped storage, respectively, while equation (19) sets an upper limit on the amount of power generated from dispatchable generators as their nameplate capacity

$$Pg_{g,b,gt,y,p} = G_{g,b,gt}^{param} CF_{b,gt,y,p} \quad \forall g \in \mathrm{G}_{curt}^{exist}, b, gt, y, p \tag{16}$$

$$Pg_{g,b,gt,y,p} = G_{g,b,gt} CF'_{b,gt,y,p} \quad \forall g \in \mathrm{G}_{curt}^{cand}, b, gt, y, p \tag{17}$$

$$Pg_{g,b,gt,y,p} = G_{g,b,gt} CF''_{b,gt,y,p} \quad \forall g, b, y, p, gt \in \{ml, ps\} \tag{18}$$

$$Pg_{g,b,gt,y,p} \leq G_{g,b,gt,y} \quad \forall g \in \mathrm{G}^{disp}, b, gt, y \tag{19}$$

Generation curtailment constraints. Equations (20) to (24) allow for generation curtailment, or a reduction in power produced by a particular curtailable generator for a specific block b

$$\Phi_{g,b,gt,y,p} = 0 \quad \forall g \in \mathrm{G}^{disp}, b, gt, y, p \tag{20}$$

$$\Phi_{g,b,gt,y,p} \le Pg_{g,b,gt,y,p} \quad \forall g \in \mathrm{G}^{curt}, b, gt, y, p \tag{21}$$

$$\begin{aligned}&\Phi_{g,b,gt,y,p} \le Pg_{g,b,gt,y,p}\\&\quad \text{if } gt = ps \text{ and } G^{param}_{g,b,gt} CF_{b,gt,y,p} > 0\end{aligned} \tag{22}$$

$$\begin{aligned}&\Phi_{g,b,gt,y,p} = 0\\&\quad \text{if } gt = ps \text{ and } G^{param}_{g,b,gt} CF_{b,gt,y,p} \le 0\end{aligned} \tag{23}$$

$$\Phi_{g,b,gt,y,p} = 0 \quad \text{if } gt = ml \tag{24}$$

Reserve constraint (one for BPA and one for outside BPA). Reserve equations (25) and (26) lead to building more generation than that needed to meet peak load. The model includes only two planning reserve regions, one that includes all the buses contained within the BPA's operational area and one for the rest of the WI

$$\sum_{g,b,gt} (CC_{gt} G_{g,b,gt,y}) + \eta_y \ge R_m \sum_b (D^{Peak}_{b,y}) \quad \forall y, b \in \mathrm{B}' \tag{25}$$

$$\sum_{g,b,gt} (CC_{gt} G_{g,b,gt,y}) + \eta_y \ge R_m \sum_b \left(D^{Peak}_{b,y}\right) \quad \forall y, b \in \mathrm{B}'' \tag{26}$$

Existing line KVL, limits, and reference angle. Transmission equations (27) to (32) model power flows in existing lines which adhere to KVL—meaning that these are existing alternating current (AC) transmission lines. Flow limits in equations (28) and (29) are line limits based on thermal capacity, while line limits (equations (30) and (31)) force the phase angle across a line to be less than $\neq / 6$ or 30 degrees

$$X_l f_{l_{b,b'},y,p} = \theta_{b,y,p} - \theta_{b',y,p} \quad \forall l \in L^E_{l'}, y, p \tag{27}$$

$$f_{l_{b,b'},y,p} \le f_l^{Max} \quad \forall l \in L^{Ep}_{l'}, y, p \tag{28}$$

$$f_{l_{b',b},y,p} \ge -f_l^{Min} \quad \forall l \in L^{Ep}_{l'}, y, p \tag{29}$$

$$f_{l,y,p} \le \frac{\pi}{6X_l} \quad \forall l_{b,b'} \in L^{Eq}_{l'}, y, p \tag{30}$$

$$f_{l,y,p} \ge -\frac{\pi}{6X_l} \quad \forall l_{b,b'} \in L^{Eq}_{l'}, y, p \tag{31}$$

$$\theta_{b_0,y,p} = 0 \text{ for some } b_0 \in \mathrm{B} \text{ and } \forall y, p \tag{32}$$

Existing line limits not adhering to KVL. Transmission equations (33) and (34) model power flows in existing lines which do not adhere to KVL—meaning that these are DC lines

$$f_{l_{b,b'},y,p} \leq f^{Max}_{l_{b,b'}} \quad \forall l_i \in L^E_l, y, p \tag{33}$$

$$f_{l_{b',b},y,p} \geq -f^{Min}_{l_{b,b'}} \quad \forall l_i \in L^E_l, y, p \tag{34}$$

Candidate line limits not adhering to KVL. The simulation uses a hybrid transmission model for candidate AC lines, since this avoids integer decision variables which can greatly increase the computational time. As such, KVL is relaxed for candidate transmission lines as indicated by equations (35) to (38). The factors of 2^{n-1} in equations (35) and (36) are the result of the model formulation being developed to solve both linear and mixed integer programs (MIPs) where binary variables represent the decision to build a transmission line in the MIP. In an MIP, it is useful to minimize the use of binary variables as they increase computational time and introducing the concept of bundles of lines n allows large amounts of new capacity to be added to the system while reducing binary variable use. In this analysis, however, only continuous decision variables are considered so the factors of 2^{n-1} could be removed from equations (6), (35), and (36) along with the n indices so long as the right-hand side of equation (37) is changed to $\sum_{i=1}^{max(n)} 2^{i-1}$

$$f'_{l_{b,b'},y',p,n} \leq 2^{n-1} f^{Max}_{l_{b,b'}} \sum_{y<y'} \Delta L_{l,y-d,n} \quad \forall l \in L^C_l, y', p, n \tag{35}$$

$$f'_{l_{b,b'},y',p,n} \geq -2^{n-1} f^{Min}_{l_{b,b'}} \sum_{y<y'} \Delta L_{l,y-d,n} \quad \forall l \in L^C_l, y', p, n \tag{36}$$

$$\sum_{y \leq y'} \Delta L_{l,y,n} \leq 1 \quad \forall l \in L^C_l, y', n \tag{37}$$

$$\Delta L_{l,y,n} = 0 \text{ if } y = max(y) \quad \forall l, n \tag{38}$$

Path limits. Aggregate line flow limits are defined in equations (39) to (41). Path flows are often defined by transmission operators to indicate a flow limit on a group of transmission lines that may be smaller than the sum of their flow capacities

$$f^{path}_{q,y,p} = \sum_l f^{dir}_{l_{b,b'},q} f_{l_{b,b'},y,p} \quad \forall l \in L^E, y, p \tag{39}$$

$$f^{path}_{q,y,p} \leq f^{path,max}_q \quad \forall q, y, p \tag{40}$$

$$f^{path}_{q,y,p} \geq -f^{path,min}_q \quad \forall q, y, p \tag{41}$$

Kirchhoff's Current Law. Transmission and generation models are connected through Kirchhoff's Current Law (KCL; equation (42)) which ensures that the sum of all power injections at each bus is zero

$$\begin{aligned} &\sum_{l_{b',b} \in L_l^E} (f_{l_{b',b},y,p}) - \sum_{l_{b,b'} \in L_l^E} (f_{l_{b,b'},y,p}) \\ &+ \sum_{l_{b',b} \in L_l^C} (f'_{l_{b',b},y,p,n}) - \sum_{l_{b,b'} \in L_l^C} (f'_{l_{b,b'},y,p,n}) \\ &+ \sum_{g,gt} (Pg_{g,b,gt,y,p}) - \sum_{g,gt} (\Phi_{g,b,gt,y,p}) \\ &= Pd_{b,y,p} - D_{b,y,p}^{Shed} \quad \forall b, y, p \end{aligned} \tag{42}$$

Load shedding upper bound. Equation (43) sets an upper bound to the amount of load shedding allowed at any bus in the model. This is equivalent to the demand minus motor loads (which are negative) minus pumped storage when it is acting as a load (meaning it is negative)

$$\begin{aligned} D_{b,y,p}^{Shed} \le Pd_{b,y,p} &- \sum_{g,gt=ml} (Pg_{g,b,gt,y,p}) \\ &- \sum_{g,gt=ps} (Pg_{g,b,gt,y,p} 1_{(Pg_{g,b,gt,y,p} \le 0)}) \quad \forall b, y, p \end{aligned} \tag{43}$$

Discount rate and end effects. Appropriate model discounting to achieve a net present value is contained in equations (44) and (45)

$$\xi_y = \left(\frac{1}{1+r}\right)^{y-min(y)} \tag{44}$$

$$\xi'_y = \sum_{x=0}^{(d-1)+24\cdot 1_{y=max(y)}} \left(\frac{1}{1+r}\right)^x \quad \forall y \tag{45}$$

Methods

The WI system

The network used for this study is a 312-bus transmission representation of the WI (Figure 1); however, the area of interest is the BPA operational area. The system topology and network data are obtained from the WECC 2024 TEPPC Common Case (WECC, 2014a) using a Kron reduction (Zhu and Tylavsky, 2017). Graphical service layer credits in Figure 1 are attributed to Esri et al. (2018).

Operational blocks

Computational complexity prohibits simulating the planning horizon for all 8760 hours of each year of the planning horizon. To accommodate this, a netload clustering algorithm utilizing MATLAB's implementation of the *k*-medoids algorithm (MathWorks, 2016) is used to determine characteristic hours appropriate for simulation. Netload based on forecasted loads and existing generation profiles for each year y, block p, and bus b is defined by

Figure 1. WI system map. Green circles represent BPA buses and red squares represent buses outside the BPA area.
Service Layer Credits: Sources: Esri, HERE, DeLorme, Intermap, increment P Corp., GEBCO, USGS, FAO, NPS, NRCAN, GeoBase, IGN, Kadaster NL, Ordnance Survey, Esri Japan, METI, Esri China (Hong Kong), swisstopo, MapmyIndia, © OpenStreetMap contributors, and the GIS User Community.

$$\begin{aligned} NL_{y,p,b} &= load_{y,p,b} - wind_{y,p,b} - solar_{y,p,b} \\ &\quad - hydro_{y,p,b} - pumped\ storage_{y,p,b} \end{aligned} \tag{46}$$

For the simulations in section "Results," 44 hours of WI peak netload is initially assigned to a single block and the remaining 8716 hours is used in the netload clustering algorithm to determine 19 additional characteristic netload blocks for a total of 20 operational blocks per simulation year.

For each year, a matrix with one row corresponding to each of the remaining 8716 hours and one column corresponding to each bus with nonzero netload is produced. The *k*-medoids algorithm receives this as input and outputs *k* medoids where each medoid serves as the most representative point of its cluster. The hour corresponding to each medoid is used to select parameter values for each block p such as load ($Pd_{b,y,p}$) and characteristic outputs ($CF_{b,gt,y,p}$, $CF'_{b,gt,y,p}$, $CF''_{b,gt,y,p}$) from their remaining 8716 hours profiles. The number of points or hours in each medoid's cluster is used to determine the number of hours $hr_{y,p}$ each block accounts for in the simulation. In this way, we capture the system's peak netload condition as well as determine an additional 19 representative hours each weighted by the number of hours that have similar features to approximate the full 8760 hours of the year.

Wind and solar profiles

Existing wind plant production is represented from the WECC 2024 TEPPC Common Case (WECC, 2014a). Production for candidate wind is based on a data set called the Wind Toolkit produced by the National Renewable Energy Laboratory (NREL; Draxl et al., 2015). This dataset characterizes wind at 100 m hub height throughout the entire United States at a resolution of $2 \times 2\,km^2$ based on modeling of 2007–2013 conditions using the Weather Research and Forecasting (WRF) numerical weather prediction model. Each site is identified with a node in the network model, based on proximity. For each wind investment node in the WI, capacity potential for wind investment is identified for three wind resource quality bins: high, medium, and low. The quantity of available capacity in each bin at a specific node is based on the wind quality at the node's geographical location. Wind investments can be made using class 1, 2, and 3 turbine technologies in order of increasing capital cost, increasing power in lower wind speed conditions (due to larger rotors), and decreasing high-end cut-out speeds (and so having decreasing production in higher wind speed conditions). Thus, for each node, there are nine possible investment options associated with the three resource quality bins and the three turbine technologies. In Tables 3, 6, and 9, these are indicated by WC*i*B*j* where *i* represents the class ($i=1$ denotes the least expensive class) and *j* represents the quality bin ($j=1$ denotes the highest quality).

Solar production from existing solar plants is represented using data from the WECC 2024 TEPPC Common Case (WECC, 2014a). Production for candidate solar is based on a new data set called the National Solar Radiation Database (NSRDB; Habte et al., 2017) using the Physical Solar Model. As described in (NSRDB; Habte et al., 2017), this model produces gridded solar irradiance at $4 \times 4\,km^2$ spatial resolution and half hour time resolution from 1998 to 2015 while power generation profiles are obtained using the NREL System Advisor Model ((Blair et al., 2014)).

Generation costs

All the existing generator data come from WECC 2024 Common Case (WECC, 2014a). For candidate wind and solar, resource hourly availability and capital costs are obtained from the NREL Annual Technology Baseline workbook (NREL, 2016). For conventional generation candidates (gas combined cycle and gas combustion turbine), the capital cost, fixed operation and maintenance (O&M) cost, and variable O&M cost come from WECC's capital cost tool (WECC, 2014b). For biomass and geothermal, all data come from the Capital Cost Review of Generation Technologies (Olsen et al., 2014) and WECC 2014 capital cost tool. All capital costs vary geographically. Generation fuel prices are taken from the 2024 WECC Common Case.

Candidate transmission

Costs are adapted from the 2014 WECC Capital Costs for Transmission and Substations Report (WECC, 2014c) with several modifications to aid in an automated line development process. For each of the 650 existing AC WI lines, a candidate is generated. DC lines are not considered for expansion. If the AC line is a preserved line, then a candidate of identical voltage class and capacity is generated with a cost based strictly on the distance of the line. The cost per mile is assumed to be 2, 1.35, and 1 million dollars per mile for 500-, 345-, and 230-kV lines, respectively. For any line less than 0.1 miles, a distance of 0.1 miles is used to determine the line cost in order to prevent zero cost lines. If an existing AC line is an equivalent line, the process is identical to that above except that instead of using the existing line's capacity a new line capacity is calculated typical of the new line candidate's voltage class and length. Because the database contained several lines with nonstandard voltage classes such as 287 and 300 kV, the cost and capacities of these lines were estimated using data from 230- and 345-kV lines, respectively.

In the scenario where the Kron reduction results in an existing line connected to buses with different voltage classes, a line is developed using the higher voltage class and the transformer costs are estimated and added to the line costs as described above using costs of 10,350, 11,400, and 13,400 dollars per MVA for 230/345-, 230/500-, and 345/500-kV transformers, respectively. Terrain factors, conductor multipliers, transmission structure type, transmission length cost multipliers, reconductor multipliers, and right-of-way costs listed in WECC (2014c) are not used in estimating line candidate costs for this work. WECC (2014c) is only used to obtain reasonable costs per mile and costs per MVA for standard transmission voltage classes and transformers, respectively. Industry contacts have indicated that the transmission costs as estimated are likely low. As such, a sensitivity analysis is performed in section "Results" that doubles all the costs listed above.

High-voltage direct current (HVDC) transmission lines are a potentially important technology for future transmission expansion and the model used in this work is capable of considering them (see equations (35) to (38)). Here, however, we have chosen to neglect them in this study to reduce the model complexity assuming that, by doing so, we are not substantially affecting the conclusions of the study.

End effects

A challenging modeling issue in finite approximations of infinite length planning horizons is how to terminate the planning horizon while still getting similar investments as that of an infinite length planning horizon. When the planning horizon is terminated in a fashion that produces results that can only be explained by the abrupt termination of a planning horizon, we refer to these as "end effects."

One approach to reduce end effects in expansion planning involves fixing the operations and investments in the final year of the simulation but costing the operations of the final year as if it were 30+ years. In this work, this is achieved through the logical operator 1_y in equation (45).

Simulation setup

The planning horizon for the simulation is 2014–2032 where investment decisions are made in the years 2014, 2020, and 2026. An additional 30 years is added to the simulation with identical parameter values as 2032 to account for end effects. Investments go into operation 6 years after the decision has been made to build them corresponding to the years 2020, 2026, and 2032. Within the planning horizon, operational decisions are replicated for the years 2014–2019, 2020–2025, 2026–2031, and 2032–2061.

Software and hardware

The model is formulated as a linear program in GAMS (GAMS Development Corporation, 2015) and solved using CPLEX (International Business Machines Corp., 2016). All simulations are run using servers with 128 GB of memory and two Intel(R) Xeon(R) CPU E5-2650 0 @ 2.00GHz for a total 16 cores. The simultaneous cooptimization problems had solution times ranging from ~0.5 to ~10.5 hours while the cumulative solution times for serially solving 10 iterations of GEP and TEP problems ranged from ~6 to ~11.5 hours.

Maps throughout this article were created using ArcGIS® software by Esri. ArcGIS® and ArcMap™ are the intellectual property of Esri and are used herein under license. Copyright © Esri. All rights reserved. For more information about Esri® software, please visit www.esri.com (Environmental Systems Research Institute (ESRI), 2016).

Results

In this section, the difference between the cooptimization and iterative approaches using the full WI is demonstrated. Sections "Figure legends" and "Definitions" provide figure legend information and definitions. Section "Simultaneous versus iterative cooptimization sensitivity studies" provides numerical and graphical results.

Figure legends

In Figures 3 to 5, lines represent transmission capacity investments where thickness represents the amount of line capacity. The different symbols represent generation capacity investment where size represents the amount of capacity in MW (Figure 2). In the following simulations, only wind, solar, natural gas combined cycle (Gas CCGT), and natural gas combustion turbines (Gas CT) receive investments (Figures 2 to 5). Figures 2 to 5 graphical service layer credits are attributed to Esri et al. (2018)

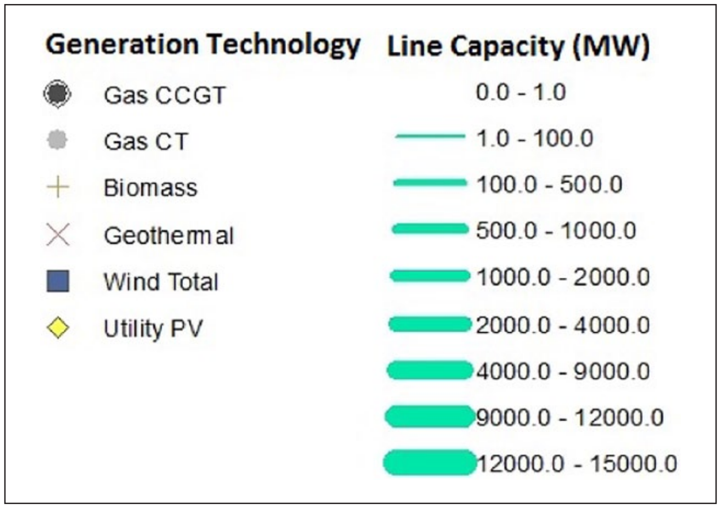

Figure 2. Line/generation investment legend for Figures 3 to 5. Generated with ArcGIS (Environmental Systems Research Institute (ESRI), 2016).

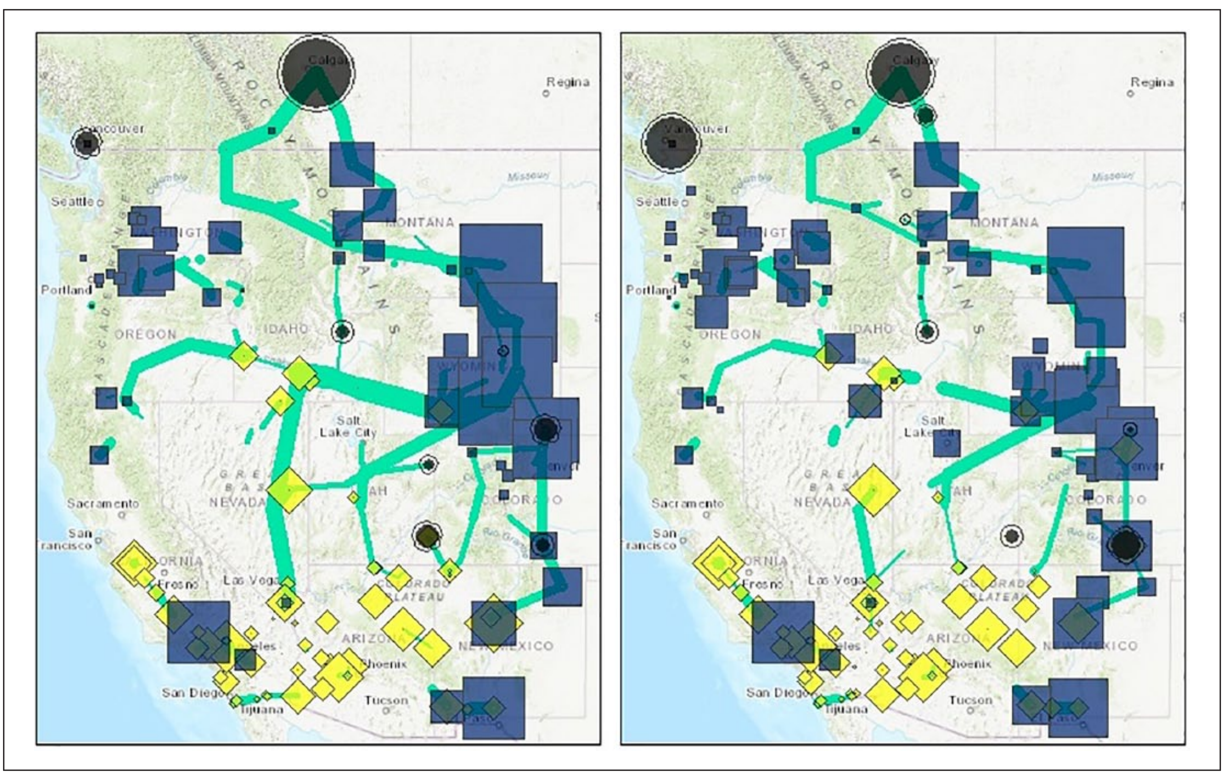

Figure 3. Case 1: cooptimized approach (left) and iterative approach (right)—10 iterations, cumulative investments 2032.
Service Layer Credits: Sources: Esri, HERE, DeLorme, Intermap, increment P Corp., GEBCO, USGS, FAO, NPS, NRCAN, GeoBase, IGN, Kadaster NL, Ordnance Survey, Esri Japan, METI, Esri China (Hong Kong), swisstopo, MapmyIndia, © OpenStreetMap contributors, and the GIS User Community.

Definitions

Two quantities in Tables 2, 5, and 8 that warrant further explanation include cooptimization benefit (column 4) and transmission benefit captured (column 5). The cooptimization benefit is the cost of the plan at the end of a sequential approach iteration minus the cost of the simultaneous cooptimized plan.

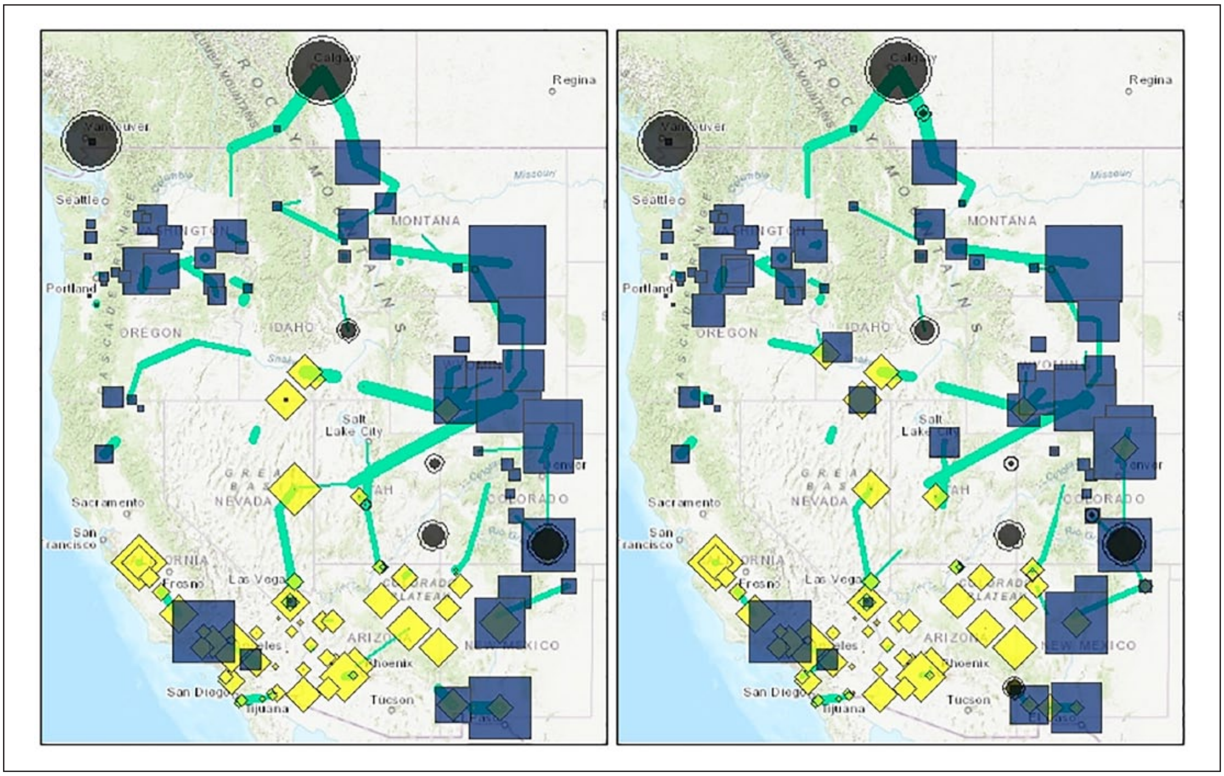

Figure 4. Case 2: cooptimized approach (left) and iterative approach (right)—10 iterations, cumulative investments 2032.
Service Layer Credits: Sources: Esri, HERE, DeLorme, Intermap, increment P Corp., GEBCO, USGS, FAO, NPS, NRCAN, GeoBase, IGN, Kadaster NL, Ordnance Survey, Esri Japan, METI, Esri China (Hong Kong), swisstopo, MapmyIndia, © OpenStreetMap contributors, and the GIS User Community.

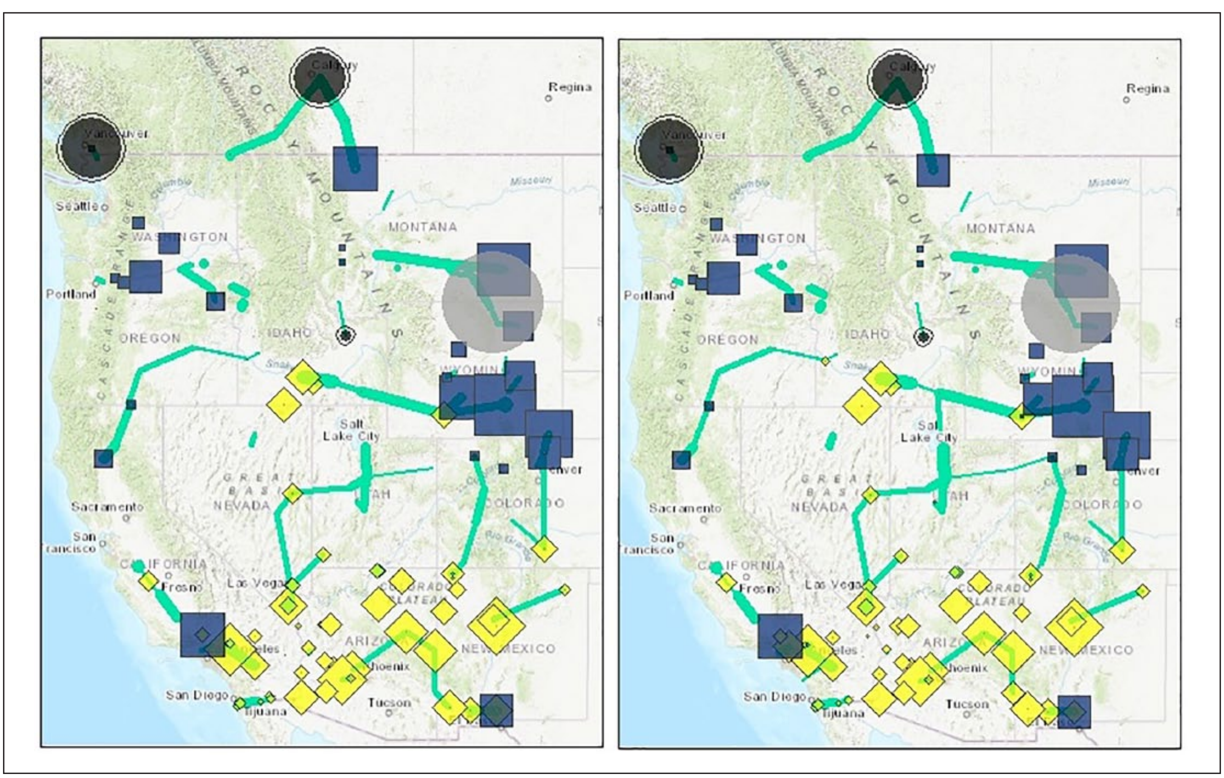

Figure 5. Case 3: cooptimized approach (left) and iterative approach (right)—10 iterations, cumulative investments 2032.
Service Layer Credits: Sources: Esri, HERE, DeLorme, Intermap, increment P Corp., GEBCO, USGS, FAO, NPS, NRCAN, GeoBase, IGN, Kadaster NL, Ordnance Survey, Esri Japan, METI, Esri China (Hong Kong), swisstopo, MapmyIndia, © OpenStreetMap contributors, and the GIS User Community.

Table 2. Case 1: iterative results (all costs in million \$).

	Cooptimization Objective = \$791,462		GEPObjective = \$815,527	
Iteration	Iterative Plan Cost	Iteration i–Iteration (i–1)	Cooptimization Benefit	Trans Benefit Captured
1	810,642	NA	19,180	20%
2	805,222	−5,421	13,760	43%
3	802,732	−2,490	11,270	53%
4	801,064	−1,667	9,603	60%
5	799,923	−1,141	8,461	65%
6	799,155	−768	7,693	68%
7	798,603	−552	7,142	70%
8	798,235	−368	6,774	72%
9	797,863	−373	6,401	73%
10	797,517	−346	6,055	75%

GEP: generation expansion plan; NA: not available.

Table 3. Case 1: cumulative 2032 investment decisions.

Investment Decisions	Cooptimization	Iterative	Difference
Category	GW	GW	GW
Biomass	0.00	0.00	0.00
Gas CCGT	7.10	8.19	−1.09
Gas CT	0.00	0.00	0.00
Geothermal	0.00	0.00	0.00
Utility PV (fixed tilt)	42.34	45.90	−3.57
WC1B1	16.01	13.84	2.18
WC1B2	7.20	5.24	1.96
WC1B3	4.15	0.44	3.71
WC2B1	23.93	27.98	−4.05
WC2B2	18.37	12.63	5.74
WC2B3	6.97	2.39	4.58
WC3B1	2.03	2.79	−0.75
WC3B2	0.00	0.00	0.00
WC3B3	0.00	0.00	0.00
Wind Total	78.68	65.31	13.37
Gen Total	128.12	119.40	8.71
Trans Total	308.59	146.22	162.37

CCGT: combined cycle gas turbine; CT: combustion turbine; PV: photovoltaic.

The transmission benefit captured is the same used in Spyrou et al. (2017). The denominator of this quantity is equivalent to the cost difference in the GEP (no transmission allowed) and TEP (simultaneous cooptimization). The numerator is equal to the cost of the GEP minus the iterative plan cost. The percent of transmission benefit captured is then the numerator divided by the denominator where only the iterative plan cost in the numerator varies by iteration.

In addition, for Tables 2, 5, and 8, row 1 indicates cooptimization objective function and GEP objective function with transmission fixed. Then in row 2, Column 1 gives iteration number, column 2 indicates iterative plan cost for each iteration, and column 3 indicates the difference between rows in column 2.

Simultaneous versus iterative cooptimization sensitivity studies

The three simulation sensitivities are described below. The state/regional wind energy analysis is contained in Table 11.

Table 4. Case 1: cost of investment in the BPA area. Carbon cost is $58/ton.

Millions of Dollars	Cooptimize	Iterative	Diff
Generation	16,020	22,421	−6,401
Transmission	2,427	825	1,603
VOM	3,287	3,450	−164
FOM	16,261	18,531	−2,270
Fuel	19,866	21,114	−1,248
Carbon	10,471	11,199	−729
Total	68,332	77,541	−9,208

BPA: Bonneville Power Administration; VOM: variable operating and maintenance; FOM: fixed operating and maintenance.

Table 5. Case 2: iterative results (all costs in million $).

	Cooptimization Objective = $801,923		GEPObjective = $815,527	
Iteration	Iterative Plan Cost	Iteration i– Iteration (i–1)	Cooptimization Benefit	Trans Benefit Captured
1	811,631	NA	9,708	29%
2	807,483	−4,148	5,560	59%
3	805,991	−1,492	4,068	70%
4	805,181	−810	3,259	76%
5	804,460	−722	2,537	81%
6	803,924	−536	2,001	85%
7	803,698	−226	1,775	87%
8	803,538	−160	1,615	88%
9	803,376	−162	1,453	89%
10	803,270	−106	1,347	90%

GEP: generation expansion plan; NA: not available.

Table 6. Case 2: cumulative 2032 investment decisions.

Investment Decisions	Cooptimization	Iterative	Difference
Category	GW	GW	GW
Biomass	0.00	0.00	0.00
Gas CCGT	8.60	9.00	−0.39
Gas CT	0.00	0.00	0.00
Geothermal	0.00	0.00	0.00
Utility PV (fixed tilt)	45.31	45.16	0.15
WC1B1	14.86	13.71	1.16
WC1B2	5.35	5.13	0.22
WC1B3	0.35	0.00	0.35
WC2B1	22.24	25.49	−3.25
WC2B2	14.82	12.14	2.68
WC2B3	2.15	2.10	0.05
WC3B1	2.19	2.74	−0.55
WC3B2	0.00	0.00	0.00
WC3B3	0.00	0.00	0.00
Wind Total	61.97	61.30	0.67
Gen Total	115.88	115.46	0.42
Trans Total	133.32	108.19	25.13

CCGT: combined cycle gas turbine; CT: combustion turbine; PV: photovoltaic.

Table 7. Case 2: cost of investment in the BPA area. Carbon cost is $58/ton and transmission costs doubled.

Millions of Dollars	Cooptimize	Iterative	Diff
Generation	18,211	21,266	−3,054
Transmission	479	317	162
VOM	3,484	3,514	−31
FOM	17,037	18,122	−1,086
Fuel	21,446	21,706	−260
Carbon	11,439	11,606	−167
Total	72,096	76,532	−4,436

BPA: Bonneville Power Administration; VOM: variable operating and maintenance; FOM: fixed operating and maintenance.

Table 8. Case 3: iterative results (all costs in million $).

	Cooptimization Objective = $624,351		GEPObjective = $628,893	
Iteration	Iterative Plan Cost	Iteration i–Iteration (i–1)	Cooptimization Benefit	Trans Benefit Captured
1	626,060	NA	1,709	62%
2	625,010	−1,050	659	85%
3	624,847	−163	496	89%
4	624,732	−114	382	92%
5	624,649	−84	298	93%
6	624,604	−44	254	94%
7	624,581	−24	230	95%
8	624,565	−15	215	95%
9	624,552	−13	201	96%
10	624,539	−13	188	96%

GEP: generation expansion plan; NA: not available.

Case 1. Cooptimized versus iterative approach (10 iterations)—with carbon costs $58 per metric ton; iterative approach summarized in Table 2; and end-year (2032) investments for both cooptimized and iterative approaches illustrated in Figure 3 and summarized in Table 3. BPA costs are summarized in Table 4.

Case 2. Cooptimized versus iterative approach (10 iterations)—with carbon costs $58 per metric ton and all base transmission/transformer costs doubled; iterative approach summarized in Table 5; and end-year (2032) investments for both cooptimized and iterative approaches illustrated in Figure 4 and summarized in Table 6. BPA costs are summarized in Table 7.

Case 3. Cooptimized versus iterative approach (10 iterations)—with carbon costs $18 per metric ton; iterative approach summarized in Table 8; and end-year (2032) investments for both cooptimized and iterative approaches illustrated in Figure 5 and summarized in Table 9. BPA costs are summarized in Table 10.

Discussion

As expected, for each scenario, the cooptimized approach outperforms the iterative approach in terms of cost. The maximum transmission benefits, or cost difference between the cooptimized approach and a single GEP, are given by approximately 24.1, 13.6, and 4.5 billion dollars, while the iterative approach only obtains 75%, 90%, and 96% of this benefit after 10 iterations for cases 1–3, respectively. At the end of 10 iterations, none of the three iterative approaches have converged, but the simulation with the lowest carbon cost appears to have captured the highest percentage of transmission benefit. As observed, when carbon costs decrease or transmission costs increase, remote resources such as wind become less economic. The benefit of cooptimization decreases from ~6.1 to ~0.2 billion dollars for decreased carbon costs and to 1.3 billion dollars for increased transmission costs after 10 iterations.

Transmission benefit captured for the scenarios studied (as defined in section "Definitions") at the end of 10 iterations is in the range of approximately $75\%-96\%$ indicating that cooptimization identifies much more effective use

Table 9. Case 3: cumulative 2032 investment decisions.

Investment Decisions	Cooptimization	Iterative	Difference
Category	GW	GW	GW
Biomass	0.00	0.00	0.00
Gas CCGT	6.58	7.05	−0.47
Gas CT	10.58	10.40	0.18
Geothermal	0.00	0.00	0.00
Utility PV (fixed tilt)	35.14	35.20	−0.06
WC1B1	6.75	5.68	1.07
WC1B2	4.43	4.38	0.05
WC1B3	0.00	0.00	0.00
WC2B1	11.20	10.24	0.96
WC2B2	0.04	0.03	0.02
WC2B3	1.99	1.99	0.00
WC3B1	0.04	0.04	0.00
WC3B2	0.00	0.00	0.00
WC3B3	0.00	0.00	0.00
Wind Total	24.45	22.35	2.10
Generation Total	76.76	75.01	1.74
Transmission Total	105.00	99.61	5.39

CCGT: combined cycle gas turbine; CT: combustion turbine; PV: photovoltaic.

Table 10. Case 3: cost of investment in the BPA area. Carbon cost is $18/ton.

Millions of Dollars	Cooptimize	Iterative	Diff
Generation	3,415	3,415	0
Transmission	111	104	7
VOM	2,988	3,005	−17
FOM	11,836	11,836	0
Fuel	17,505	17,631	−126
Carbon	4,164	4,195	−31
Total	40,019	40,185	−167

BPA: Bonneville Power Administration; VOM: variable operating and maintenance; FOM: fixed operating and maintenance.

of transmission than the iterative approach. As a comparison to prior uses of this metric, Spyrou et al. (2017) find the value of approximately $14\%-89\%$ for their iterative approach studies. It is interesting to note that, while Spyrou et al. (2017) find convergence using the iterative approach, sometimes in just a few iterations this study does not within the 10 iterations allotted. This might be attributed to Spyrou et al. (2017) using binary transmission investment variables as opposed to the continuous transmission investment variables used in this study. Initially, in this study, we attempted to use binary transmission investment variables, but the problem quickly became intractable for even a single iteration given that there are 650 candidate transmission lines, each being allowed to expand up to 15 times its single line capacity.

General trends included increased wind and transmission capacity investments in the cooptimized approach in comparison to the iterative approach. Since wind and transmission capacity investments are lower in the iterative approach this likely signals a greater use of existing generation or local investments such as natural gas or photovoltaic (PV). In all sensitivities, the iterative approach yields more natural gas technology investments. In cases 1 and 3, the iterative approach results in more solar PV investments.

While simultaneous cooptimization guarantees costs at least as low as the iterative approach, costs associated with a grid partition, in contrast to solving for investments in the entire interconnection, may actually be higher. In all three simulations, the cooptimization benefit in the column "Difference" and row "Total" of Tables 4, 7, and 10 is larger than the cooptimization benefit of the WI in Tables 2, 5, and 8. This implies that the cost of infrastructure investments located outside of the BPA area is actually higher in cooptimization than in the iterative approach.[1]

Table 11. Cumulative GW investment of wind by state/region (C, I, and D represent cooptimization, iterative, and difference, respectively, for the different carbon cost scenarios).

	$58			58T			$18		
	C	I	D	C	I	D	C	I	D
AZ	0.0	0.0	0.0	0.0	0.0	0.0	0.0	0.0	0.0
BC	0.1	0.1	0.0	0.1	0.1	0.0	0.0	0.0	0.0
CA	4.6	4.7	0.0	4.7	4.7	0.0	2.3	2.3	0.0
CFE	0.0	0.0	0.0	0.0	0.0	0.0	0.0	0.0	0.0
CO	4.7	7.0	−2.3	5.9	7.3	−1.3	1.1	1.1	0.0
ID	0.0	2.0	−2.0	0.1	1.7	−1.6	0.0	0.0	0.0
MT	11.3	10.8	0.5	9.9	9.6	0.2	4.8	3.9	0.9
NV	0.0	0.0	0.0	0.0	0.0	0.0	0.0	0.0	0.0
NM	8.3	8.8	−0.6	8.7	8.7	0.0	1.1	1.0	0.1
OR	5.7	7.2	−1.5	6.2	6.8	−0.6	1.6	1.6	0.0
UT	0.0	0.7	−0.7	0.0	0.8	−0.8	0.0	0.0	0.0
WA	2.6	4.4	−1.8	3.2	4.2	−1.0	0.5	0.5	0.0
WY	41.4	19.6	21.8	23.2	17.5	5.8	13.0	11.8	1.2
Total	78.7	65.3	13.4	62.0	61.3	0.7	24.5	22.4	2.1

One explanation for lower costs associated with the buses in the BPA area is that less infrastructure investments are made within the BPA area (meaning less operational costs in the BPA area). Instead, high-capacity factor remote resources are used to support BPA operations. This hypothesis is supported by Tables 4, 7, and 10 as far greater generation investment and operational costs occur in the iterative approaches than for the cooptimized approach.

Finally, in Table 11, the state/regional effects of cooptimization on wind investment are displayed. In case 1, it is observed that cooptimization increases wind investment in MT and WY, while wind investment is static or decreases in all other areas. In case 3, if wind is disadvantaged by reducing the carbon costs, then after 10 iterations the difference in the cooptimization and sequential approaches appears to be almost entirely due to increases in wind in WY and MT, while other state investments vary slightly between approaches. On the other hand, if wind is disadvantaged by higher transmission costs in case 2, then after 10 iterations wind investment is only $\sim 700\,\mathrm{MW}$ higher in the cooptimized case. However, the actual location of the wind investment between the approaches is quite different. The cooptimized approach contains ~6 GW more wind investment in MT and WY and ~5 GW less wind investment in all the other states. Thus, each of the sensitivities supports the view that cooptimization enables higher capacity factor wind investments found in remote locations such as MT and WY.

Conclusion

In this article, the effect of simultaneously cooptimizing generation and transmission is compared against sequentially solving the GEP and TEP for 10 iterations. The investments of the simulations are illustrated pictorially and analyzed at three different system levels: at the interconnection level, at the regional utility (BPA) level, and at the individual state level.

The analysis at each of the three levels indicates that simultaneous cooptimization outperforms sequential cooptimization in identifying transmission-supported remote resources that result in lower overall costs. This is best observed in the cases 1 and 2 where simultaneous cooptimization results in (1) greater system wind installations, (2) reduced BPA wind installations in WA, OR, and ID, (3) increased remote wind installations in MT and WY, (4) greater system transmission capacity investments, and (5) greater BPA transmission costs. In case 3, all of these trends are observed except for (2) after 10 iterations.

Industry planning today is usually well characterized by sequential cooptimization, where frequently a generation facility is planned and transmission is subsequently developed to support that project. Sometimes, the GEP is then reviewed and adjusted to more appropriately utilize the planned transmission. This study shows that this approach may miss the available economic opportunities that more effectively integrate generation and transmission expansion plans, particularly opportunities that involve supplying loads from high-quality resources that are remote from those loads.

Acknowledgements

The authors would like to thank The Bonneville Power Administration and The National Science Foundation for making this work possible.

Declaration of conflicting interests

The author(s) declared no potential conflicts of interest with respect to the research, authorship, and/or publication of this article.

Funding

The work presented herein was funded in part by the Bonneville Power Administration under Award No. 67110. The views and opinions of the authors expressed herein do not necessarily state or reflect those of the US Government or any agency thereof. This work was also performed under NSF Awards 1069283 and 1408401.

Note

1. The model employed in this study attributes cost to bus location which is not what occurs in reality. FERC order 1000 attributes cost to causation. In other words, cost is attributed to the party that causes it regardless of where it is located.

References

Adams N, Beglari F, Laughton M, et al. (1972) Mathematical programming systems in electrical power generation, transmission and distribution planning. In: *Proceedings of the 4th power systems computational conference*, Grenoble, 11–16 September.

Berrie T and Anderson D (1972) Power system planning, development programs and project selection—a discussion of methods. In: *Proceedings of the 4th power systems computational conference*, Grenoble, 11–16 September.

Blair N, Dobos A, Freeman J, et al. (2014) *System advisor model, SAM 2014.1.14: General description*. Technical report NREL/TP-6A20-61019. Golden, CO: National Renewable Energy Laboratory.

Draxl C, Hodge B, Clifton A, et al. (2015) *Overview and meteorological validation of the wind integration national dataset toolkit*. Technical report NREL/TP-5000-61740. Golden, CO: National Renewable Energy Laboratory.

Environmental Systems Research Institute (ESRI) (2016) *ArcGIS Release 10.4.1*. Redlands, CA: Environmental Systems Research Institute.

Esri, HERE, DeLorme, et al. Updated 2018 (created 2013) "Topographic" [basemap].Scale varies by Figure. *"World Topographic Map,"* 2018. Available at: https://www.arcgis.com/home/item.html?id=30e5fe3149c34df1ba922e6f5bbf808f

GAMS Development Corporation (2015) *General Algebraic Modeling System (GAMS) Release 24.5.6*. Washington, DC: GAMS Development Corporation.

Garver L (1970) Transmission network estimation using linear programming. *IEEE T Power Ap Syst* 89(7): 1688–1697.

Gu Y, McCalley JD and Ni M (2012) Coordinating large-scale wind integration and transmission planning. *IEEE T Sustain Energ* 3(4): 652–659.

Habte A, Sengupta M and Lopez A (2017) *Evaluation of the National Solar Radiation Database (NSRDB): 1998-2015*. Technical report NREL/TP-5d00-6722. Golden, CO: National Renewable Energy Laboratory.

International Business Machines Corp. (2016) *IBM ILOG CPLEX 12.7*. Armonk, NY: International Business Machines Corp.

Liu A, Hobbs BF, McCalley JD, et al. (2013) Co-optimization of transmission and other supply resources. *Technical report*. Available at: http://pubs.naruc.org/pub/536D834A-2354-D714–51D6-AE55F431E2AA

Liu Y, Sioshansi R and Conejo A (2017) Multistage stochastic investment planning with multistage representation of uncertainties and decision. *IEEE T Power Syst* 33(1): 781–791.

Maloney P and McCalley J (2017) Long term planning model value of stochastic solution and expected value of perfect information calculations with uncertain wind parameters. In: *Proceedings of the North American power symposium*, Morgantown, WV, 17–19 September 2017.

Maloney P, Olatujoye O, Ardakani AJ, et al. (2016) A comparison of stochastic and adaptation programming methods for long term generation and transmission co-optimization under uncertainty. In: *Proceedings of the North American power symposium*, Denver, CO, 18–20 September 2016.

Masse P and Gibrat R (1957) Application of linear programming to investments in the electric power industry. *Manage Sci* 3: 149–166.

MathWorks (2016) MATLAB and Statistics and Machine Learning Toolbox Release 2016a. Natick, MA: MathWorks.

Munoz FD, Hobbs BF, Ho JL, et al. (2014) An engineering-economic approach to transmission planning under market and regulatory uncertainties: WECC case study. *IEEE T Power Syst* 29(1): 307–317.

National Renewable Energy Laboratory (2016) NREL annual technology baseline workbook. Technical report, National Renewable Energy Laboratory, Golden, CO. Available at: https://data.nrel.gov/submissions/52 (accessed on 16 September 2016).

Olsen R, Schlag N, Patel K, et al. (2014) Capitol cost review of generation technologies. Technical report, Energy and Environmental Economics, Inc. Available at: https://www.wecc.biz/Reliability/2014_TEPPC_Generation_CapCost_Report_E3.pdf.

Sasson AM and Merrill HM (1974) Some applications of optimization techniques to power system problems. *Proc IEEE* 62(7): 959.

Spyrou E, Ho JL, Hobbs BF, et al. (2017) What are the benefits of co-optimizing transmission and generation investment? Eastern Interconnection Case Study. *IEEE T Power Syst* 32(6): 4265–4277.

WECC (2014a) 2024 Common Case v1.5. Technical report, WECC. Available at: https://www.wecc.biz/Reliability/2024-Common-Case.zip (accessed on 29 April 2015)

WECC (2014b) WECC, 2014 TEPPC generation capital cost calculator. Technical report, WECC. Available at: https://www.wecc.biz/Reliability/E3_WECC_ProForma_FINAL.xlsm (accessed on 31 Jan 2017)

WECC (2014c) WECC, 2014 TEPPC transmission capital cost report. Technical report, WECC. Available at: https://www.wecc.biz/Reliability/2014_TEPPC_TransCapCostCalculator.xlsx (accessed on 14 March 2016)

Xu Q and Hobbs BF (2017) Johns Hopkins stochastic multi-stage integrated network expansion (JHSMINE). *Technical report, Johns Hopkins University*. Available at: http://hobbsgroup.johnshopkins.edu/home.html

Zhu Y and Tylavsky D (2017) An optimization-based dc-network reduction method. *IEEE T Power Syst* 3(3): 2509–2517.

Author biographies

Patrick Maloney is a PhD student at Iowa State University co-majoring in Wind Energy Science Engineering and Policy and Electrical Engineering. Prior to starting his PhD, he earned an MS is Electrical Engineering at the University of Wisconsin – Madison in 2010 and a BA in Physics at Carleton College in Northfield, MN, USA in 2007. His PhD research focuses on long-term generation and transmission cooptimization planning under uncertainty.

Ping Liu received the BS and MS degrees in Electrical Engineering from Southwest Jiaotong University, Sichuan, China in 2007 and 2010, respectively. Upon finishing the PhD degree in Electrical Engineering at Mississippi State University, she did a 1-year postdoc at Lawrence Berkeley National Laboratory and a 2-year postdoc at Iowa State University. Currently, she is working at ABB Enterprise Software, Atlanta, GA, USA. Her research interests include power system planning and operation, energy market simulation, and distributed energy resources integration.

Qingyu Xu is a doctoral student in Environmental Engineering at Johns Hopkins University. His research expertise focuses on power markets and co-optimization of electricity transmission generation and storage. He has received an MS in Environmental Engineering from Johns Hopkins University in 2015 after a BS in Ecology from Sun Yat-Sen University, Guangzhou, China in 2013.

James D McCalley received the BS, MS, and PhD degrees from the Georgia Institute of Technology, Atlanta, GA, USA, in 1982, 1986, and 1992, respectively. He was a transmission planning engineer for PG&E, San Francisco, CA, USA during 1985–1990. Since 1992, he has been with the Electrical and Computer Engineering Department, Iowa State University, Ames, IA, USA, where he is currently a Distinguished Professor. He is a fellow of the IEEE.

Benjamin F Hobbs is the Theodore M. and Kay W. Schad Chair of Environmental Management at the Johns Hopkins University and has been a member of the faculty of that university's Department of Environmental Health & Engineering since 1995. He earned a PhD in Environmental Systems Engineering in 1983 from Cornell University, and his research addresses systems and economic analyses of power and environmental systems. Most recently, his research has focused on transmission planning, market design, and short-term forecasting for renewables integration. Previously, he was at Brookhaven and Oak Ridge National Laboratories, and on the faculty of Case Western Reserve University. Since 2010, he has been the Director of the JHU Environment, Energy, Sustainability & Health Institute; he also co-directs the USEPA Yale-JHU SEARCH (Solutions for Energy, Air, Climate, and Health) Center. He chairs the Market Surveillance Committee of the California Independent System Operator. He is a fellow of IEEE and INFORMS.

Sara Daubenberger is an Electrical Engineer in the Bonneville Power Administration's Long Term Planning group. Her study focus includes commercial power flow studies and long-range capacity expansion models. In 2004, she joined the Bonneville Power Administration as an Electrical Engineer in the Transmission Operations department, running power flow studies to set system operating limits and dispatch support. She graduated from the University of Portland with a Bachelors in Electrical Engineering in 2004 and received her Masters of Science in Electrical Engineering from Portland State University in 2005.

Anders Johnson is an Electrical Engineer in the Bonneville Power Administration's Long Term Planning group. He enjoys exploring complex problems and developing innovative solutions. He has a broad range of power systems analysis expertise in power flow, integrated resource and transmission planning, security-constrained economic dispatch, short circuit analysis, and electromagnetic transients. He also has experience in technology innovation and transmission line permitting. He has represented BPA on the NERC Planning Committee and WECC Scenario Development Subcommittee.

Stan Williams received a Masters of Science in Forestry and Operations Research from Texas A&M University. He worked for 5 years in Integrated Resource Planning at PacifiCorp starting in 2004. In 2009, he joined Bonneville Power Administration and now works in long-term transmission planning.